Lamellar Inorganic Ion Exchangers. Hydrogen–Lithium Ion Exchange in γ-Titanium Phosphate

Eliana González, Ricardo Llavona, José R. García, and Julio Rodríguez*
Area de Química Inorgánica, Facultad de Química, Universidad de Oviedo, Oviedo, Spain

The ion-exchange process of H^+ and Li^+ in γ-titanium phosphate (γ-TiP) was studied. Exchange isotherms and titration and hydrolysis curves were obtained at 25.0, 40.0, and 55.0 (±0.1) °C by using LiCl + LiOH solutions. The ion-exchange process and the thermal behaviour of the exchanged solids were monitored by *X*-ray diffraction. The exchanged phases $TiH_{1.5}Li_{0.5}(PO_4)_2 \cdot 2H_2O$ (interlayer distance 11.0 Å), $TiHLi(PO_4)_2 \cdot 2H_2O$ (11.3 Å), and $TiHLi(PO_4)_2$ (9.6 Å) were detected. At > 200 °C the $TiH_{1.5}Li_{0.5}(PO_4)_2 \cdot 2H_2O$ phase transformed into mixtures of the $Ti(HPO_4)_2$ (9.1 Å) and $TiHLi(PO_4)_2$ phases. Extents of conversion higher than 50% with high decomposition of γ-TiP were obtained. The equilibrium constant, free energy, enthalpy, and entropy of the exchange reactions are reported.

Phosphates of quadrivalent metals with lamellar structure can be used as ionic exchangers.[1] Their structure resembles that of clay minerals[2–4] but the systems here are much simpler.

The α phases, $M(HPO_4)_2 \cdot H_2O$, have been widely studied, mainly those of zirconium and titanium (α-ZrP and α-TiP),[5–9] but their interlayer spacings are rather small (7.6 Å)[10,11] and this fact restricts the diffusion of highly hydrated cations.[12–15]

The γ phases of these materials (γ-ZrP and γ-TiP) have a greater basal spacing (12.2 and 11.6 Å respectively) and their composition is $M(HPO_4)_2 \cdot 2H_2O$.[16,17] This large interlayer distance suggests an easier ionic diffusion of large cations. However, their ion-exchange properties have been scarcely studied.

The behaviour of an ion exchanger in binary systems (H^+,M^+; M = alkaline metal) gives useful information which can be used to explain more complicated systems. These binary systems have been widely studied in γ-ZrP[18] but in γ-TiP only the retention of Na^+[17,19] and K^+[20,21] has been reported, despite the fact that this material shows good exchange properties with NH_4^+, Cu^{2+}, or Ca^{2+} ions.[22–25]

This paper reports the results obtained in a study of H^+/Li^+ ion exchange in γ-TiP. For the sake of brevity, the various ionic forms are simply indicated by their counter ions (under a bar) and water contents, while their interlayer distances are reported in parentheses.

Experimental

Reagents.—All chemicals used were of reagent grade. γ-Titanium bis(hydrogenphosphate) was obtained by using 16.5 mol dm^{-3} H_3PO_4 and a reflux time of 10 d as previously described.[26]

Analytical Procedures.—The concentrations of phosphorus and titanium in the solids were determined gravimetrically.[27] The pH measurements were made with an Orion model SA-720 pH meter. The phosphate groups released were measured spectrophotometrically[28] using a Perkin-Elmer model 200 instrument. The Li^+ in solution was determined by atomic absorption spectroscopy, using a Perkin-Elmer model 372 spectrometer. Thermal gravimetric analysis (t.g.a.) and differential thermal analysis (d.t.a.) were performed by a Chio model TRDA-3H instrument. The diffractometer used was a Philips model PV 1050/23 (λ = 1.7902 Å, 2θ scan rate 0.125—2° min^{-1}, chart speed 2 cm min^{-1}).

Ion-exchange Studies.—The exchanger was equilibrated with LiCl + LiOH solutions at 25.0, 40.0, and 55.0 (±0.1) °C using the procedure described by Clearfield *et al.*[29] The solutions were prepared with constant amounts of 0.04 mol dm^{-3} LiCl and increasing amounts of LiOH in such a manner that the ionic strength at equilibrium is constant if the exchange process behaves ideally. The equilibration time was 48 h. The solid was present in the solution in the ratio of *ca.* 1 g:250 cm^3.

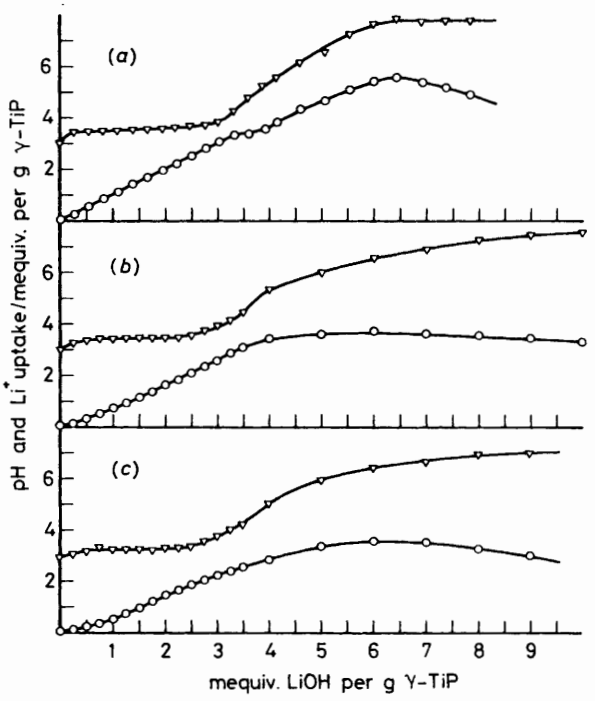

Figure 1. Exchange isotherms (○) and pH curves (▽) of γ-TiP at 25.0 (*a*), 40.0 (*b*), and 55.0 °C (*c*)

Results and Discussion

Figure 1 shows exchange isotherms and pH curves plotted against the amount of LiOH added. It can be observed that the equilibrium pH remains constant for additions of 0.5—2.5 mequiv. LiOH per g γ-TiP at the three working temperatures. When the LiOH concentration is greater than 3.0 mequiv. per g γ-TiP in the initial solutions, the equilibrium pH increases and reaches values between 6.8 and 7.8 when the initial

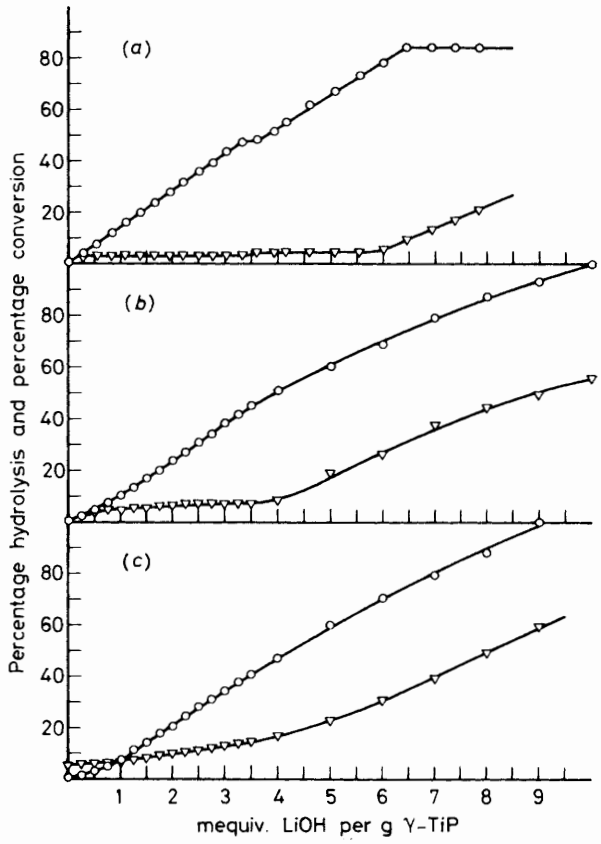

Figure 2. Hydrolysis curves (▽) and exchange isotherms corrected for hydrolysis (○) at 25.0 (*a*), 40.0 (*b*), and 55.0 °C (*c*)

concentration of LiOH concurs with the exchange capacity of γ-TiP (7.25 mequiv. per g).

The exchange isotherms are qualitatively similar at the three temperatures and the retention of Li^+ initially increases with the amount of LiOH added. The highest retention corresponds to additions of 5.5—7.0 mequiv. LiOH per g γ-TiP and this value decreases with temperature: 5.5 (25.0), 3.8 (40.0), and 3.5 mequiv. per g (55.0 °C). Greater concentrations of LiOH lead to a decrease in the retention.

The shape of the isotherms indicates that the ion-exchange process coexists with partial decomposition of the exchanger due to the presence of hydroxyl groups in solution. The hydrolysis can be expressed by equations (1) or (2) depending

$$Ti(HPO_4)_2{\cdot}2H_2O + 4OH^- + (n-4)\,H_2O \longrightarrow TiO_2{\cdot}nH_2O + 2HPO_4^{2-} \quad (1)$$

$$Ti(HPO_4)_2{\cdot}2H_2O + 2OH^- + (n-2)\,H_2O \longrightarrow TiO_2{\cdot}nH_2O + 2H_2PO_4^- \quad (2)$$

on the pH of the equilibrium solution.[30] Quantitative analysis of phosphorus in the equilibrium solutions (see Experimental section) allows the percentage hydrolysis of γ-TiP to be obtained (Figure 2). The hydrolysis increases with temperature and with the concentration of LiOH in the initial solutions.

Figure 2 shows the corrected exchange isotherms, in which the substitution is expressed as a percentage of the total exchange capacity of the mass of γ-TiP not hydrolyzed. The saturation of γ-TiP at 55.0 °C is reached with the addition of 9.0 mequiv. LiOH per g, while 10.0 mequiv. LiOH per g are needed at 40.0 °C and the maximum conversion reached at 25.0 °C is about 85%.

The solid, after its separation from the equilibrium solution, is dried in air at room temperature. The *X*-ray diffraction behaviour is shown in Figure 3(*a*). In the range of $0.00 < \overline{X} < 0.25$ (where $\overline{X}$ is the molar fraction of exchange defined as the fraction of hydrogens substituted in γ-TiP) the presence of two reflections is observed in the region of the interlayer distance [Figure 4(*a*)], one of them (corresponding to the 002 plane of γ-TiP) appears at 11.6 Å and the other at 11.0 Å. The intensity of the latter reflection increases with increasing conversion. The reflection characteristic of γ-TiP is not observed when $\overline{X} = 0.25$. *X*-Ray patterns of intermediate samples may be reproduced by combination of the patterns corresponding to the limiting samples, showing the coexistence of two crystalline phases in this composition range.

Thermal analysis of the 25% substitution sample, stabilized in air [Figure 5(*a*)], shows the existence of two different zones of mass loss. The former, at temperatures < 200 °C, corresponds to 2 mol H_2O per mol Ti. This zone of temperature is associated with the loss of crystallization water in this kind of compound.[31,32] Moreover, the d.t.a. curve shows two minima at 95 and 170 °C which indicate that the dehydration takes place in two steps as in γ-TiP.[26] The material again loses mass at higher temperatures (300—550 °C) as a consequence of condensation of the hydrogenphosphate groups into pyrophosphate ones. The minima in the d.t.a. curve at 310 and 460 °C suggest that this dehydration also takes place in two steps. A similar behaviour of γ-TiP was explained by La Ginestra and Massucci[32] as the formation of an intermediate phosphate/pyrophosphate phase with an interlayer distance of 8.3 Å. A sharp maxima appears in the d.t.a. curve at higher temperatures (637 °C) whilst the material weight hardly varies at > 600 °C. An exothermic peak was also detected for γ-TiP at 880 °C corresponding to the transformation of α-TiP_2O_7 into a high-temperature phase. The presence of Li^+ in the interlayer spacing of γ-TiP gives rise to a strong decrease in the temperature corresponding to the phase change.

In Table 1 are compiled the *X*-ray diffraction data for the crystalline phase $\overline{H_{1.5}Li_{0.5}}{\cdot}2H_2O$ (11.0 Å).

A detailed study of the *X*-ray patterns of solids with $0.25 < \overline{X} \leqslant 0.50$, stabilized in air at room temperature [Figure 3(*a*)], shows several variations in the rest of the pattern despite the fact that the interlayer distance hardly changes (11.0—11.3 Å) with increasing conversion. When $\overline{X} = 0.50$ there are no reflections characteristic of the $\overline{H_{1.5}Li_{0.5}}{\cdot}2H_2O$ (11.0 Å) phase. These results suggest the existence of a defined crystalline phase of half-exchange.

Thermal analysis of a sample at 50% substitution stabilized in air [Figure 5(*b*)] indicates that the dehydration behaviour of this sample is similar to that of the 25% exchanged phase. There is a loss of mass corresponding to 2 mol of H_2O per mol of Ti at < 250 °C which, in this case, takes place in three steps, with minima in the d.t.a. curve at 75, 125, and 170 °C. At 400—600 °C, a second loss of mass occurs with a minimum in the d.t.a. curve at 460 °C. There is a sharp maximum in the d.t.a. curve at higher temperatures (622 °C) which does not correspond to a weight loss as was the case for the 25% substitution phase (d.t.a. sharp maximum at 637 °C). The increase in the concentration of Li^+ in the interlayer spacing of γ-TiP facilitates the phase change.

The difficulty in obtaining conversions higher than 50% may be explained by assuming that γ-TiP has two hydrogen ions in each zeolitic cavity and, thus, the counter ions should be in very close proximity in the totally exchanged phases and the electrostatic repulsive forces between them should be very high. Moreover, the formation of 25% substitution phases[19,20] suggests the existence of two different zeolitic cavities in γ-TiP. If we take into account the transformation during the thermal treatment of the 25% substitution phases into mixtures of

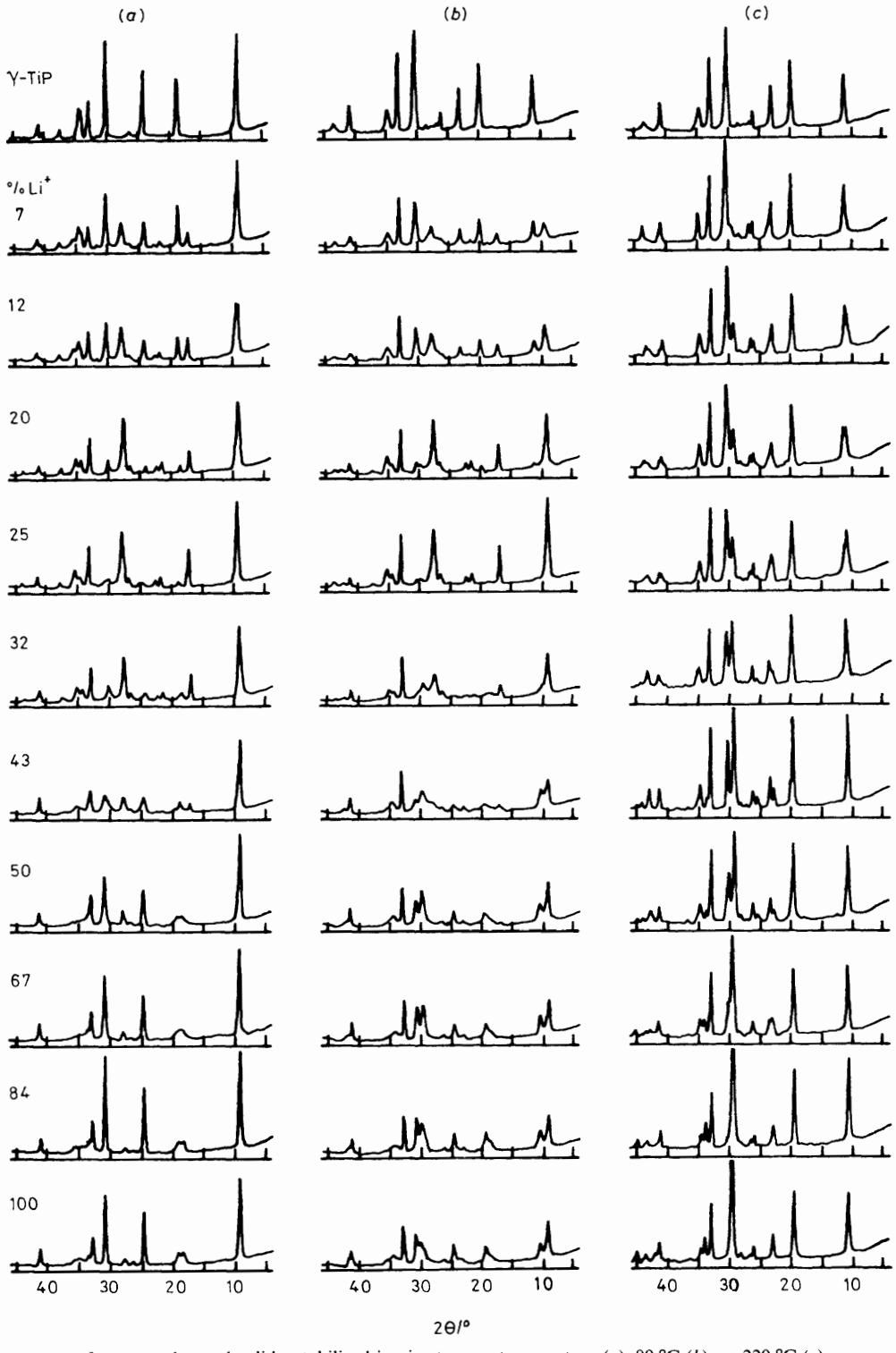

Figure 3. *X*-Ray patterns of some exchanged solids, stabilized in air at room temperature (*a*), 80 °C (*b*), or 220 °C (*c*)

unchanged phases and half-exchanged phases, we can assume that the two different types of zeolitic cavities are placed in alternative interlayer spacings.

In the $\overline{HH}\cdot 2H_2O$ (11.6 Å) and $\overline{H_{1.5}Li_{0.5}}\cdot 2H_2O$ (11.0 Å) phases the condensation of the hydrogenphosphate into pyrophosphate groups takes place in two steps. Nevertheless, the condensation of the $\overline{HLi}\cdot 2H_2O$ (11.3 Å) phase occurs only in one step whose minimum in the d.t.a. curve concurs with the temperature characteristic of the second step in the condensation of the $\overline{HH}\cdot 2H_2O$ (11.6 Å) and $\overline{H_{1.5}Li_{0.5}}\cdot 2H_2O$ (11.0 Å) phases. This suggests that the ionic substitution until 50% exchange in γ-TiP affects the hydrogen ions of the hydrogenphosphate groups whose condensation into pyrophosphate takes place more easily.

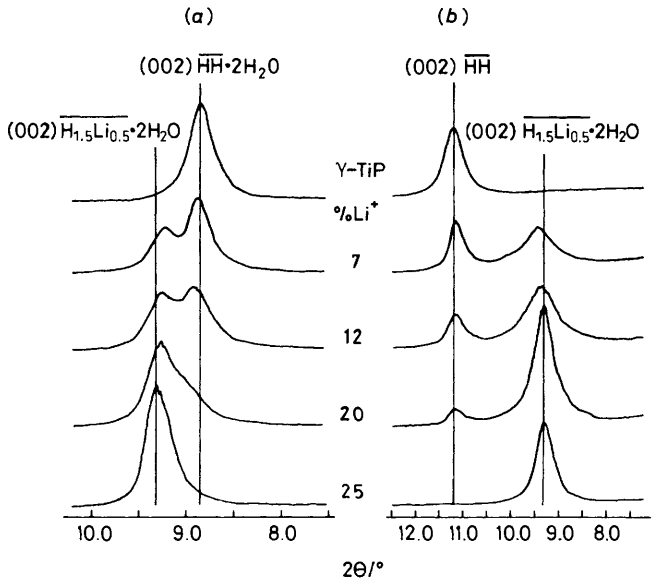

Figure 4. *X*-Ray diffraction lines corresponding to the interlayer distance of some exchanged solids, stabilized in air at room temperature (*a*) or 80 °C (*b*)

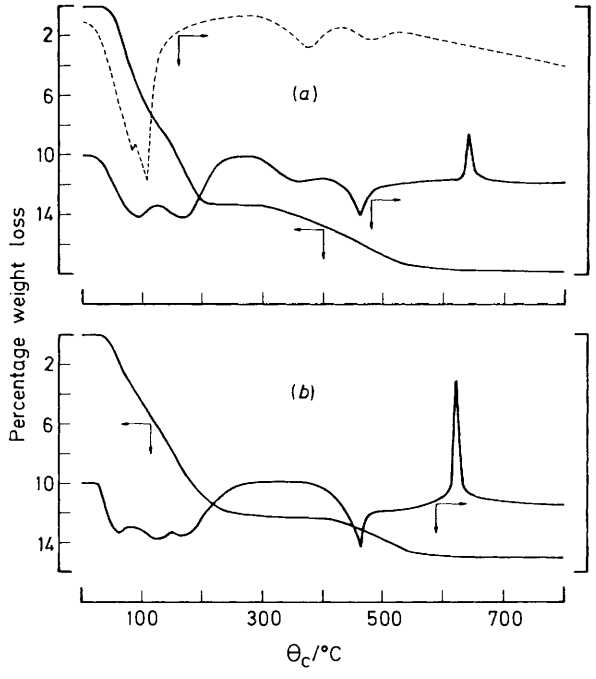

Figure 5. D.t.a. and t.g.a. curves of the $\overline{H_{1.5}Li_{0.5}}$·2H$_2$O (*a*) and $\overline{HLi}$·2H$_2$O (*b*) phases. The dashed line represents the d.t.a. curve of γ-TiP (ref. 26)

In Table 1 are collected the *X*-ray diffraction data of crystalline phases $\overline{HLi}$·2H$_2$O (11.3 Å) and $\overline{HLi}$ (9.6 Å).

Figure 3(*a*) shows *X*-ray patterns of solids with $\bar{X} > 0.50$ stabilized in air at room temperature. The substitution occurs without change in the patterns. The existence of defined crystalline phases with intermediate composition is not detected during the transformation of the half-exchanged phase into the total exchanged phase.

Table 1. *X*-Ray diffraction data for exchanged phases

$\overline{H_{1.5}Li_{0.5}}$·2H$_2$O		$\overline{HLi}$·2H$_2$O		$\overline{HLi}$	
d/Å	*I*/%	*d*/Å	*I*/%	*d*/Å	*I*/%
11.0	100	11.3	100	9.6	80
6.01	45	5.61	10	5.27	85
4.77	10	5.37	10	4.54	15
4.58	5	4.21	40	4.43	30
4.20	5	3.74	15	4.06	5
4.12	5	3.38	50	3.95	20
3.87	10	3.15	30	3.55	100
3.73	60	2.54	15	3.43	55
3.14	50			3.15	80
3.02	10			3.00	15
2.95	20			2.54	15
2.77	5			2.46	15
2.53	10				

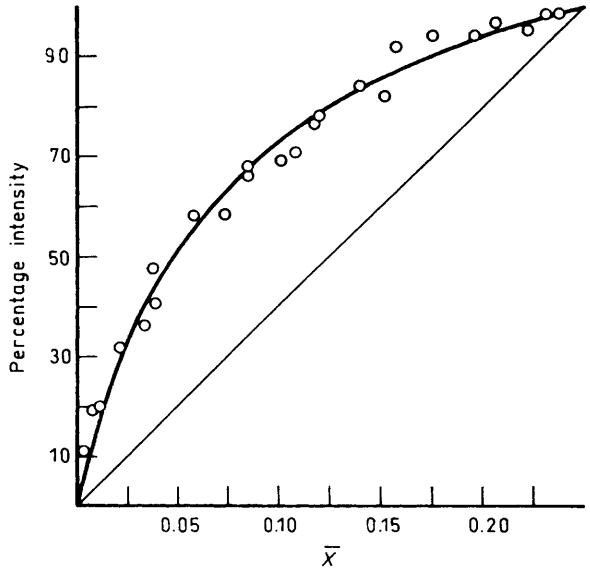

Figure 6. Variation of the intensity of the reflection corresponding to the interlayer distance of $\overline{H_{1.5}Li_{0.5}}$·2H$_2$O (11.0 Å) relative to that of the $\overline{HH}$ (9.1 Å) phase

X-Ray patterns of the exchanged solids heated at 80 °C are collected in Figure 3(*b*). For $0.00 < \bar{X} < 0.25$ there is coexistence of the characteristic reflections of the $\overline{HH}$ (9.1 Å) and $\overline{H_{1.5}Li_{0.5}}$·2H$_2$O (11.0 Å) phases, in good agreement with the thermal behaviour of the crystalline phases present in the solids.

The difference between the interlayer distances of the crystalline phases present in the samples stabilized at 80 °C is relatively great and this fact enables quantitative data to be obtained by *X*-ray diffraction by measuring the relative intensity of the reflections associated with the 002 planes of these phases [Figure 4(*b*)].

Lamellar compounds are notorious for exhibiting preferred orientations, which affects intensity measurements in *X*-ray diffraction.[33] Errors in such measurements are minimized by grinding the γ-TiP to a particle size smaller than 30 μm, by dividing each sample into five portions, and obtaining the average value of the corresponding five determinations. The variation of the relative intensity (determined by cutting out the peak areas and weighing them) of the phases present under the reported conditions is plotted in Figure 6.

In lamellar materials, the concentration (C_j) of a crystalline phase j in a mixture is a linear function of its relative intensity (I_j) [equation (3)],[34,35] where f_j is a constant for each crystalline phase. The molar fraction of exchange will be given by equation (4). From this, equation (5) is deduced.

$$C_j = f_j I_j \tag{3}$$

$$\bar{X} = \tfrac{1}{4}\frac{f_{\overline{H_{1.5}Li_{0.5}}} I_{\overline{H_{1.5}Li_{0.5}}}}{f_{\overline{HH}} I_{\overline{HH}} + f_{\overline{H_{1.5}Li_{0.5}}} I_{\overline{H_{1.5}Li_{0.5}}}} \tag{4}$$

$$\frac{f_{\overline{H_{1.5}Li_{0.5}}}}{f_{\overline{HH}}} = \frac{4\bar{X}}{1-4\bar{X}} \cdot \frac{I_{\overline{HH}}}{I_{\overline{H_{1.5}Li_{0.5}}}} \tag{5}$$

By application of expression (5) to the data collected in Figure 6, $f_{\overline{H_{1.5}Li_{0.5}}\cdot 2H_2O}/f_{\gamma\text{-TiP}} = 0.25$ is obtained. These data allow the direct transformation of intensity into concentrations and give a rapid method for the determination of the saturation degree of γ-TiP.

When $\bar{X} > 0.25$, X-ray diffraction patterns of samples stabilized at 80 °C [Figure 4(*b*)] give little information about their composition because of the coexistence of two reflections in the zone of the interlayer distance over the entire composition range indicates the presence of more than one degree of hydration in phases with the same ionic content.

Heating at 220 °C for 72 h of the exchanged solids produces anhydrous materials. X-Ray patterns of the solids calcined at 220 °C [Figure 3(*c*)] show an evolution by degrees from $\bar{X} =$ 0.00 to 0.50. Although the existence of a definite crystalline phase at 25% substitution might be expected, no discontinuity is observed. The patterns of the samples with $0.00 < \bar{X} < 0.50$ can be reproduced from those corresponding to the $\overline{HH}$ (9.1 Å) and $\overline{HLi}$ (9.6 Å) phases. A detailed study of the interlayer distance zone (Figure 7) reveals (despite the angular proximity of the bands characteristic of the basal spacing of both crystalline phases) the decrease in intensity of the β-TiP reflection (9.1 Å), at the same time as the conversion increases toward the reflection corresponding to the $\overline{HLi}$ (9.6 Å) phase, both coexisting at $\bar{X} = 0.25$. The behaviour of the 25% conversion phase when heated at 220 °C can be explained only by the existence of thermal splitting, already detected in other phases of partial substitution in γ-TiP.[19,20,25,33] The process is summarized in equation (6).

$$2\overline{H_{1.5}Li_{0.5}}\cdot 2H_2O\ (11.0\ \text{Å}) \longrightarrow \overline{HH}\ (9.1\ \text{Å}) + \overline{HLi}\ (9.6\ \text{Å}) \tag{6}$$

When $\bar{X} > 0.50$, the X-ray patterns of the solids treated at 220 °C [Figure 3(*c*)] give little information. The interlayer distance of the material remains constant over the entire composition range, small variations in the rest of the pattern being observed.

A systematic study of ion-exchange materials requires thermodynamic data for the substitution reactions. The two first steps of the exchange process referred to 1 mol of exchanger can be expressed in the forms (7) and (8) respectively. By making

$$Ti(HPO_4)_2\cdot 2H_2O\ (c) + \tfrac{1}{2}Li^+\ (aq) + (n-2)H_2O \rightleftharpoons TiH_{1.5}Li_{0.5}(PO_4)_2\cdot nH_2O\ (c) + \tfrac{1}{2}H^+\ (aq) \tag{7}$$

$$TiH_{1.5}Li_{0.5}(PO_4)_2\cdot nH_2O + \tfrac{1}{2}Li^+\ (aq) + (n'-n)H_2O \rightleftharpoons TiHLi(PO_4)_2\cdot n'H_2O\ (c) + \tfrac{1}{2}H^+\ (aq) \tag{8}$$

certain assumptions as in previous works, thermodynamic data for the direct exchange process can be obtained.[36,37]

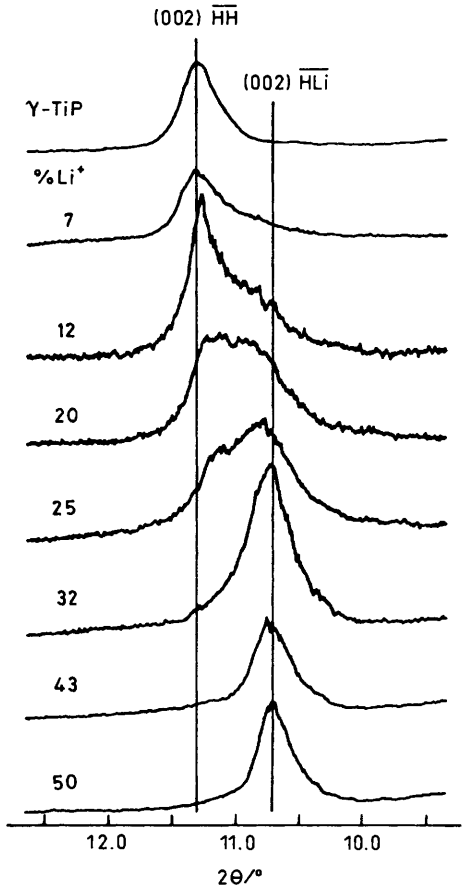

Figure 7. X-Ray diffraction lines corresponding to the interlayer distance of some exchanged solids, stabilized at 220 °C

As discussed previously,[23] expressing the exchange processes in the forms (7) and (8) has the advantage of indicating the composition of the solid crystalline phases involved and the 'real' exchange capacity of the exchanger in the substitution step considered. Equilibrium quotients can be defined in the forms (9) and (10) respectively. The quantities with bars represent the

$$K_1' = (\bar{X}_{\overline{H_{1.5}Li_{0.5}}} m_H^{\frac{1}{2}} / \bar{X}_{\overline{HH}} m_{Li}^{\frac{1}{2}})(f_H/f_{Li})^{\frac{1}{2}} \tag{9}$$

$$K_2' = (\bar{X}_{\overline{HLi}} m_H^{\frac{1}{2}} / \bar{X}_{\overline{H_{1.5}Li_{0.5}}} m_{Li}^{\frac{1}{2}})(f_H/f_{Li})^{\frac{1}{2}} \tag{10}$$

species in the solid phase and those without bars the species in solution. The concentrations of the species in solid phase are expressed in terms of the corresponding molar fraction of the phase ($\bar{X}_j$). The concentration of the species in solution is expressed in terms of molalities (m) corrected by the activity coefficients in a binary solution (f).[38]

In solution, the usual standard state where the activities of the ions are equal to the corresponding molalities in solution at infinite dilution is taken. The reference state of the solvent is also as usual in that $a_w = 1$ for the pure solvent. For the solid phase we choose the reference state in which the solid is in equilibrium with an infinitely dilute solution of the counter ion.

The equilibrium quotients expressed by equations (9) and (10) are evaluable over the entire composition range. The equilibrium constants are obtained from equation (11).[23,39] The

$$\log K_i = \int_0^1 \log K_i' \, d\bar{X}_j \tag{11}$$

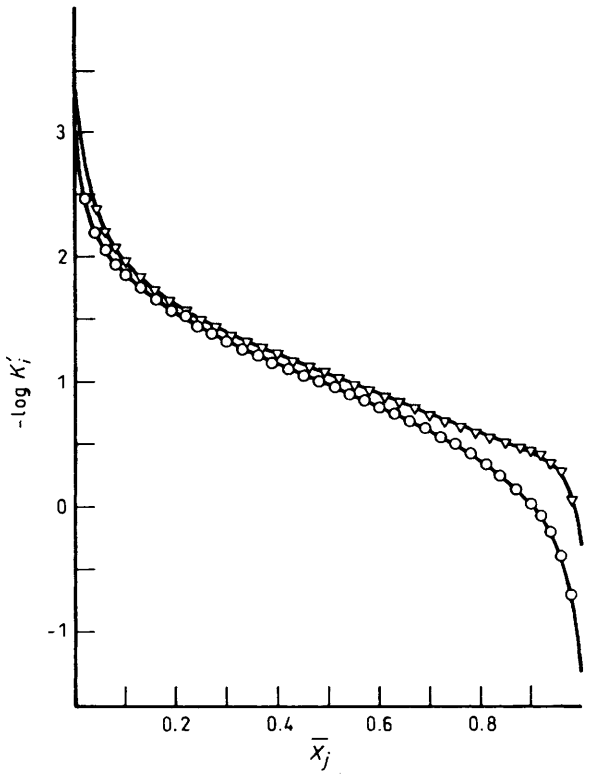

Figure 8. Plot of $-\log K_i'$ against $\bar{X}_j$ (25.0 °C) in the $\overline{HH} \rightleftharpoons \overline{H_{1.5}Li_{0.5}}$ (○) and $\overline{H_{1.5}Li_{0.5}} \rightleftharpoons \overline{HLi}$ (▽) process

integral is calculated by plotting $-\log K_i'$ against $\bar{X}_j$ and determining the area under the curve (Figure 8). By plotting the equilibrium constants against $1/T$ (Figure 9), ΔH° is obtained. By using the equations $\Delta G^\circ = -RT\ln K$ and $\Delta G^\circ = \Delta H^\circ - T\Delta S^\circ$, the values collected in Table 2 are obtained.

The enthalpy change for an exchange reaction represented by equation (7) or (8) can be thought to result from four sources:[40] (*i*) the heat consumed in bond breaking, as when H^+ is released from the exchanger; (*ii*) the heat released in the formation of bonds to the incoming cation; (*iii*) the heat corresponding to the increase or decrease of the interlayer distance; and (*iv*) the enthalpy changes accompanying hydration and dehydration in solution.

Bearing in mind that the hydrogens are mainly covalently bonded to the phosphate oxygens, the enthalpy variation (*i*) should not be significantly affected by the size of the cavity. On the other hand, the heat released in the bonding between Li^+ and the exchanger [(*ii*)] will increase as the similarity between the ion and cavity sizes increases. Moreover, it will be a function of the degree of hydration of the exchanger. When lithium ions are placed into large cavities they may be more hydrated than when they are placed into small cavities and the enthalpy variations will therefore be different in each case. Term (*iii*) should correspond to low enthalpy variations since the $\overline{HH}\cdot 2H_2O$ (11.6 Å), $\overline{H_{1.5}Li_{0.5}}\cdot 2H_2O$ (11.0 Å), and $\overline{HLi}\cdot 2H_2O$ (11.3 Å) phases show very similar interlayer spacings. The last term (*iv*) is equivalent to the enthalpy change for the hypothetical reaction represented by equation (12) for which $\Delta H = -569.3$ kJ mol^{-1}.[41] This enthalpy variation will be the same for the two processes represented by equations (7) and (8).

$$H^+(g) + Li^+(aq) \longrightarrow H^+(aq) + Li^+(g) \qquad (12)$$

Table 2. Thermodynamic data for the H^+/Li^+ ion exchange in γ-TiP

	ΔG° / kJ mol^{-1}	ΔH° / kJ mol^{-1}	ΔS° / J K^{-1} mol^{-1}
$\overline{HH} \rightleftharpoons \overline{H_{1.5}Li_{0.5}}$	5.43	7.77	8
$\overline{H_{1.5}Li_{0.5}} \rightleftharpoons \overline{HLi}$	6.31	−8.78	−51

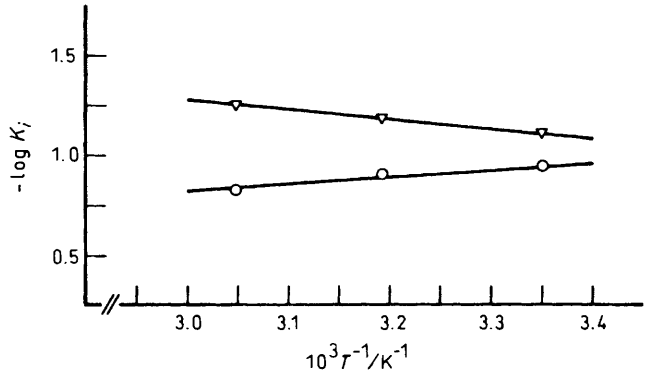

Figure 9. Influence of temperature on the equilibrium constant for $\overline{HH} \rightleftharpoons \overline{H_{1.5}Li_{0.5}}$ (○) and $\overline{H_{1.5}Li_{0.5}} \rightleftharpoons \overline{HLi}$ (▽) process

Accordingly, it is term (*ii*) which gives rise to the different ΔH values found in the 25 and 50% phase formation processes.

The enthalpy variation (Table 2) corresponds to an endothermic process in the 0—25% substitution step and to an exothermic process in the 25—50% step. Therefore, by assuming the existence of two different types of zeolitic cavities in γ-TiP, as stated before, the hydrogen ions placed in the smallest (expected to be more hydratable) zeolitic cavities will be replaced in the 0—25% step while the lithium ions will enter into the largest (less hydratable) cavities in the 25—50% step.

Although the structure of γ-TiP is so far unknown, studies performed on the exchanger, mainly regarding the thermal behaviour of the 25% exchange phases, seem to indicate the existence of two different types of zeolitic cavities, such that all the zeolitic cavities are similar to each other in interlayer spacing and different from those of the adjacent interlayer spacings. As in α-ZrP, the cavities must be connected to each other by means of small tunnels (2.64 Å in diameter in α-ZrP). According to these structural hypotheses the following substitution mechanism is proposed: lithium ions must diffuse into the solid in their anhydrous form. The heat released in the formation of bonds between the anhydrous cation and the layers of titanium phosphate will be higher, the more similar are the sizes of the cavity and the lithium ion. If both types of zeolitic cavities are able to lodge an anhydrous lithium ion without increasing the basal spacing, it might be expected that the smallest cavities would be occupied first. When all these cavities are semioccupied, the lithium ions will begin to lodge in the large cavities. The hydration of lithium ions in the zeolitic cavities will take place in a second step, to an extent which will increase with the size of the cavity.

On the basis of these considerations, the lithium half-exchanged phase should be more hydrated than the 25% substitution phase. The hydration degree of the solids obtained '*in situ*' may be different despite the fact that both have 2 mol of hydration water per mol of titanium when they are stabilized in

air. The entropy variation in the exchange reactions (Table 2) provides some information: ΔS° ($\overline{HH} \rightleftharpoons \overline{H_{1.5}Li_{0.5}}$) is small so that ion exchange does not cause noticeable variations in the solid hydration. Nevertheless, ΔS° ($\overline{H_{1.5}Li_{0.5}} \rightleftharpoons \overline{HLi}$) has a noticeable negative value related to the increase in the hydration degree of the solid during the substitution process.

The lack of knowledge concerning the crystalline structure of γ-TiP makes difficult a more extensive interpretation of these results. Nevertheless, from the variation of the standard free energy of the transformation of the $\overline{HH}$ phase into the less converted lithium phase (10.86, 14.63, and 18.70 kJ per mol of lithium for γ-TiP, α-ZrP, and α-TiP respectively[42,43]) it can be inferred that γ-TiP retains Li^+ in aqueous solution at room temperature more easily than do α-zirconium phosphate or α-titanium phosphate.

Acknowledgements

This work was supported by the Comision Asesora de Investigacion Cientifica y Tecnica (Project no. 84–0878) for which grateful acknowledgement is made.

References

1 'Inorganic Ion Exchange Materials,' ed. A. Clearfield, CRC Press, Boca Raton, Florida, 1982.
2 D. M. C. Macewan, 'The *X*-Ray Identification and Crystal Structure of Clay Minerals,' Mineralogical Society, London, 1961, ch. 4.
3 D. Leigh and A. Dyer, *J. Inorg. Nucl. Chem.*, 1972, **34**, 369.
4 F. Liebau, 'Structural Chemistry of Silicates,' Springer, Berlin, 1985.
5 V. Vesely and V. Pekarek, *Talanta*, 1972, **19**, 219.
6 'Ion Exchange and Solvent Extraction,' vol. 5, eds. J. A. Marinsky and Y. Marcus, Marcel Dekker, New York, 1973.
7 G. Alberti and U. Costantino, *J. Chromatogr.*, 1974, **102**, 5.
8 J. P. Gupta and D. V. Nowell, *Chem. Ind. (London)*, 1977, **15**, 649.
9 G. Alberti, *Acc. Chem. Res.*, 1978, **11**, 163.
10 A. Clearfield and J. A. Stynes, *J. Inorg. Nucl. Chem.*, 1964, **26**, 117.
11 G. Alberti, P. Cardini-Galli, U. Costantino, and E. Torracca, *J. Inorg. Nucl. Chem.*, 1967, **29**, 571.
12 G. Alberti, R. Bertrami, M. Casciola, U. Costantino, and J. P. Gupta, *J. Inorg. Nucl. Chem.*, 1976, **38**, 843.
13 S. E. Horsley, D. V. Nowell, and D. T. Stewart, *Spectrochim. Acta, Part A*, 1974, **30**, 535.
14 J. M. Troup and A. Clearfield, *J. Inorg. Nucl. Chem.*, 1977, **16**, 3311.
15 J. Albertsson, A. Oskarsson, R. Tellgren, and J. O. Thomas, *J. Phys. Chem.*, 1977, **81**, 1574.
16 A. Clearfield, R. H. Blessing, and J. Stynes, *J. Inorg. Nucl. Chem.*, 1968, **30**, 2249.
17 S. Allulli, C. Ferragina, A. La Ginestra, M. A. Massucci, and N. Tomassini, *J. Inorg. Nucl. Chem.*, 1977, **39**, 1043.
18 A. Clearfield and J. M. Garcés, *J. Inorg. Nucl. Chem.*, 1979, **41**, 879.
19 R. Llavona, J. R. García, C. Alvarez, M. Suárez, and J. Rodríguez, *Solvent Extr. Ion Exch.*, 1986, **4**, 567, 585.
20 R. Llavona, C. Alvarez, J. R. García, M. Suárez, and J. Rodríguez, *Solvent Extr. Ion Exch.*, 1985, **3**, 931.
21 R. Llavona, J. R. García, M. Suárez, and J. Rodríguez, *Thermochim. Acta*, 1986, **101**, 101.
22 G. Alberti, M. G. Bernasconi, M. Casciola, and U. Costantino, *J. Inorg. Nucl. Chem.*, 1980, **42**, 1637.
23 C. Alvarez, R. Llavona, J. R. García, M. Suárez, and J. Rodríguez, *J. Chem. Soc., Dalton Trans.*, 1987, 2045.
24 G. Alberti, U. Costantino, and M. L. Luciani, *J. Chromatogr.*, 1980, **201**, 175.
25 C. Alvarez, R. Llavona, J. R. García, M. Suárez, and J. Rodríguez, *Inorg. Chem.*, 1987, **26**, 1045.
26 R. Llavona, J. R. García, M. Suárez, and J. Rodríguez, *Thermochim. Acta*, 1985, **86**, 281.
27 I. M. Kolthoff, E. B. Sandell, E. J. Meehan, and S. Bruckenstein, 'Quantitative Chemical Analysis,' Nigar, Buenos Aires, 1972.
28 O. B. Michelsen, *Anal. Chem.*, 1957, **29**, 60.
29 A. Clearfield, A. Oskarsson, and C. Oskarsson, *Ion Exch. Membr.*, 1972, **1**, 91.
30 M. Suárez, J. R. García, and J. Rodríguez, *J. Phys. Chem.*, 1984, **88**, 159.
31 D. Dollimore, N. J. Manning, and D. V. Nowell, *Thermochim. Acta*, 1977, **19**, 37.
32 A. La Ginestra and M. A. Massucci, *Thermochim. Acta*, 1979, **32**, 241.
33 H. P. Klug and L. E. Alexander, '*X*-Ray Diffraction Procedures for Polycrystalline and Amorphous Materials,' Wiley, New York, 1974.
34 J. R. García, M. Suárez, C. G. Guarido, and J. Rodríguez, *Anal. Chem.*, 1984, **56**, 193.
35 R. Llavona, M. Suárez, J. R. García, and J. Rodríguez, *Anal. Chem.*, 1986, **58**, 547.
36 C. G. Guarido, M. Suárez, J. R. García, and J. Rodríguez, *J. Chem. Soc., Dalton Trans.*, 1985, 1865.
37 A. Clearfield and A. S. Medina, *J. Phys. Chem.*, 1971, **75**, 3750.
38 R. A. Robinson and R. H. Stokes, 'Electrolyte Solutions,' Butterworths, London, 1959.
39 G. L. Gaines and H. C. Thomas, *J. Chem. Phys.*, 1953, **21**, 714.
40 L. Kullberg and A. Clearfield, *J. Phys. Chem.*, 1981, **21**, 1578.
41 D. F. C. Morris, *Struct. Bonding (Berlin)*, 1968, **4**, 63.
42 C. G. Guarido, M. Suárez, J. R. García, R. Llavona, and J. Rodríguez, *J. Chem. Thermodyn.*, 1985, **17**, 63.
43 L. Kullberg and A. Clearfield, *J. Phys. Chem.*, 1981, **21**, 1585.

Received 14*th December* 1987; *Paper* 7/2174